# $|V_{us}|$ and lepton universality from kaon decays with the KLOE detector

**The KLOE Collaboration**

**F. Ambrosino,**[ef] **A. Antonelli,**[a] **M. Antonelli,**[a] **F. Archilli,**[a] **C. Bacci,**[jk] **P. Beltrame,**[b]
**G. Bencivenni,**[a] **S. Bertolucci,**[a] **C. Bini,**[hi] **C. Bloise,**[a] **S. Bocchetta,**[jk] **F. Bossi,**[a]
**P. Branchini,**[k] **R. Caloi,**[hi] **P. Campana,**[a] **G. Capon,**[a] **T. Capussela,**[a] **F. Ceradini,**[jk]
**F. Cesario,**[jk] **S. Chi,**[a] **G. Chiefari,**[ef] **P. Ciambrone,**[a] **F. Crucianelli,**[h] **E. De Lucia,**[a]
**A. De Santis,**[hi] **P. De Simone,**[a] **G. De Zorzi,**[hi] **A. Denig,**[b] **A. Di Domenico,**[hi]
**C. Di Donato,**[f] **B. Di Micco,**[jk] **A. Doria,**[f] **M. Dreucci,**[a] **G. Felici,**[a] **A. Ferrari,**[a]
**M. L. Ferrer,**[a] **S. Fiore,**[hi] **C. Forti,**[a] **P. Franzini,**[hi] **C. Gatti,**[a] **P. Gauzzi,**[hi]
**S. Giovannella,**[a] **E. Gorini,**[cd] **E. Graziani,**[k] **W. Kluge,**[b] **V. Kulikov,**[n] **F. Lacava,**[hi]
**G. Lanfranchi,**[a] **J. Lee-Franzini,**[al] **D. Leone,**[b] **M. Martemianov,**[n] **M. Martini,**[ae]
**P. Massarotti,**[ef] **W. Mei,**[a] **S. Meola,**[ef] **S. Miscetti,**[a] **M. Moulson,**[a] **S. Müller,**[a]
**F. Murtas,**[a] **M. Napolitano,**[ef] **F. Nguyen,**[jk] **M. Palutan,**[a] **E. Pasqualucci,**[i] **A. Passeri,**[k]
**V. Patera,**[ag] **F. Perfetto,**[ef] **M. Primavera,**[d] **P. Santangelo,**[a] **G. Saracino,**[ef]
**B. Sciascia,**[a] **A. Sciubba,**[ag] **A. Sibidanov,**[a] **T. Spadaro,**[a] **M. Testa,**[hi] **L. Tortora,**[k]
**P. Valente,**[i] **G. Venanzoni,**[a] **R. Versaci**[a] and **G. Xu**[am]

[a] *Laboratori Nazionali di Frascati dell'INFN,*
 *via E. Fermi 40, I-00044 Frascati, Italy*
[b] *Institut für Experimentelle Kernphysik, Universität Karlsruhe,*
 *D-76128 Karlsruhe, Germany*
[c] *Dipartimento di Fisica dell'Università,*
 *via Arnesano, I-73100 Lecce, Italy*
[d] *INFN Sezione di Lecce,*
 *via Arnesano, I-73100 Lecce, Italy*
[e] *Dipartimento di Scienze Fisiche dell'Università "Federico II",*
 *via Cintia, I-80126 Napoli, Italy*
[f] *INFN Sezione di Napoli, via Cintia, I-80126 Napoli, Italy*
[g] *Dipartimento di Energetica dell'Università "La Sapienza",*
 *P. Aldo Moro 2, I-00185 Roma, Italy*
[h] *Dipartimento di Fisica dell'Università "La Sapienza",*
 *P. Aldo Moro 2, I-00185 Roma, Italy*
[i] *INFN Sezione di Roma,*
 *P. Aldo Moro 2, I-00185 Roma, Italy*

$^j$ *Dipartimento di Fisica dell'Università "Roma Tre",*
  *via della Vasca Navale 84, I-00146 Roma, Italy*
$^k$ *INFN Sezione di Roma Tre,*
  *via della Vasca Navale 84, I-00146 Roma, Italy*
$^l$ *Physics Department, State University of New York at Stony Brook,*
  *Stony Brook, NY 11794-3840 U.S.A.*
$^m$ *Institute of High Energy Physics of Academia Sinica, Chinese Academy of Sciences,*
  *P.O. Box 918, Beijing 100049, P.R. China*
$^n$ *Institute for Theoretical and Experimental Physics,*
  *B. Cheremushkinskaya ul. 25 RU-117218 Moscow, Russia*
  *E-mail:* `paolo.franzini@lnf.infn.it`

ABSTRACT: KLOE has measured most decay branching ratios of $K_S$, $K_L$ and $K^{\pm}$-mesons. It has also measured the $K_L$ and the $K^{\pm}$ lifetime and determined the shape of the form factors involved in kaon semileptonic decays. We present in the following a description of the above measurements and a well organized compendium of all of our data, with particular attention to correlations. These data provide the basis for the determination of the CKM parameter $|V_{us}|$ and a test of the unitarity of the quark flavor mixing matrix. We also test lepton universality and place bounds on new physics using measurements of $|V_{us}|$ from $K_{\ell 2}$ and $K_{\ell 3}$ decays.

KEYWORDS: e+-e- Experiments.

# Contents

## 1. Introduction

While much emphasis is placed on the search for new physics, we still lack precise information on the validity of certain aspects of the Standard Model itself. In the Standard Model, the coupling of the $W$ boson to the weak charged current is written as

$$\frac{g}{\sqrt{2}} W_\alpha^+ (\overline{\mathbf{U}}_L \, \mathbf{V}_{\mathrm{CKM}} \gamma^\alpha \, \mathbf{D}_L + \bar{e}_L \gamma^\alpha \nu_{e\,L} + \bar{\mu}_L \gamma^\alpha \nu_{\mu\,L} + \bar{\tau}_L \gamma^\alpha \nu_{\tau\,L}) \; + \; \mathrm{h.c.}, \qquad (1.1)$$

where $\mathbf{U}^{\mathrm{T}} = (u, c, t)$, $\mathbf{D}^{\mathrm{T}} = (d, s, b)$ and $L$ is for lefthanded. In the coupling above there is only one coupling constant for leptons and quarks. Quarks are mixed by the Cabibbo-Kobayashi-Maskawa matrix, $\mathbf{V}_{\mathrm{CKM}}$, which must be unitary. In low energy processes the Fermi coupling constant $G_F$ is related to the gauge coupling $g$ by $G_F = g^2/(4\sqrt{2}\,M_W^2)$. In the early sixties only two elements of $\mathbf{V}_{\mathrm{CKM}}$ were known. From nuclear $\beta$ decay it was known that $|V_{ud}|{\sim}0.98$ and from strangeness changing decays, $|V_{us}|{\sim}0.26$, [1].
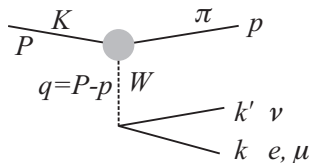
**Figure 1:** Amplitude for semileptonic kaon decay.

Precise measurements of leptonic and semileptonic kaon decay rates provide information about lepton universality. Combined with results from nuclear $\beta$ decay and pion decays, such measurements also provide information about the unitarity of the mixing matrix. Ultimately they tell us whether quarks and leptons do indeed carry the same weak charge. The universality of electron and muon interactions can be tested by measuring the ratio $\Gamma(K \to \pi\mu\nu)/\Gamma(K \to \pi e\nu)$. The partial rates $\Gamma(K \to \pi e\nu)$ and $\Gamma(K \to \pi\mu\nu)$ provide measurements of $g^4|V_{us}|^2$, which, combined with $g^4|V_{ud}|^2$ from nuclear $\beta$ decay and the muon decay rate, test the unitarity condition $|V_{ud}|^2 + |V_{us}|^2 + |V_{ub}|^2 = 1$.

In 1983 it was already known that $|V_{ub}|^2 < 4 \times 10^{-5}$ [2] and today $|V_{ub}|^2 \sim 1.5 \times 10^{-5}$ [3]. We will therefore ignore $|V_{ub}|^2$ in the following. The ratio $\Gamma(K \to \mu\nu)/\Gamma(\pi \to \mu\nu)$ provides an independent measurement of $|V_{us}|^2/|V_{ud}|^2$.

To perform these tests at a meaningful level of accuracy, radiative effects must be properly included. Strong-interactions introduce form factors, FF, which must be calculated from first principles, or measured, whenever possible. Finally, corrections for SU(2) and SU(3) breaking must also be included. Recently, advances in lattice calculations have begun to catch up with experimental progress.

## 2. What needs to be measured

### 2.1 Semileptonic kaon decays

The semileptonic kaon decay (figure 1) still provides the best means for the measurement of $|V_{us}|$, because only the vector part of the weak current contributes to the matrix element $\langle \pi | J_\alpha | K \rangle$. In general,

$$\langle \pi | \bar{u}\gamma_\alpha s | K \rangle = f_+(t)(P + p)_\alpha + f_-(t)(P - p)_\alpha, \tag{2.1}$$

where $P$ and $p$ are the kaon and pion four-momenta, respectively, and $t$ is the 4-momentum transfer squared $(P - p)^2$. The form factors (FF) $f_+$ and $f_-$ appear because pions and kaons are not point-like particles and also reflect both SU(2) and SU(3) breaking. Lorentz invariance requires the FFs to be functions only of $t$ and therefore only of the total pion energy, $E_\pi$. Since $t = (P - p)^2 = M^2 + m^2 - 2ME_\pi$, $t$ depends only, linearly, on $E_\pi$.

Introducing the scalar FF $f_0(t)$, the matrix element above is written as

$$\langle \pi(p) | \bar{u}\gamma_\alpha s | K(P) \rangle = f_+(0) \times \left( (P + p)_\alpha \, \tilde{f}_+(t) + (P - p)_\alpha \left( \tilde{f}_0(t) - \tilde{f}_+(t) \right) \frac{\Delta_{K\pi}}{t} \right), \tag{2.2}$$

with $\Delta_{K\pi} = M_K^2 - m_\pi^2$. Eq. (2.2) defines $\tilde{f}_0(t)$. The FFs $f_+$ and $f_0$ must have the same value at $t = 0$. We have therefore factored out a coefficient $f_+(0)$, so that the functions

$\tilde{f}_+(t)$ and $\tilde{f}_0(t)$ are both unity at $t = 0$. For vector transitions, the Ademollo-Gatto theorem [4] ensures that SU(3) breaking is second order in $m_s - m_{u,d}$. In fact, $f_+(0)$ differs from unity by only $\sim 4\%$. Since $P - p = k + k'$, $P - p$ dotted into the lepton term gives $m_\ell \times \bar{\ell}\,(1 - \gamma_5)\,\nu$ which can be safely neglected for $K \to \pi e \nu$ decays. Only the vector FF $\tilde{f}_+$ therefore contributes to $K_{e3}$ decays.

Assuming lepton universality, the muon decay rate provides the value of the Fermi constant, $G_F = 1.16637(1) \times 10^{-5}$ GeV$^{-2}$ [3]. The semileptonic decay rates, fully inclusive of radiation, are given by

$$\Gamma(K_{\ell3(\gamma)}) = \frac{C_K^2 G_F^2 M_K^5}{192\pi^3}\, S_{\mathrm{EW}}\, |V_{us}|^2\, |f_+(0)|^2\, I_{K\ell}\, \left(1 + \delta_K^{\mathrm{SU}(2)} + \delta_{K\ell}^{\mathrm{EM}}\right)^2. \qquad (2.3)$$

In the above expression, the index $K$ denotes $K^0 \to \pi^\pm$ and $K^\pm \to \pi^0$ transitions, for which $C_K^2 = 1$ and $1/2$, respectively. $M_K$ is the appropriate kaon mass, $S_{\mathrm{EW}}$ is the universal short-distance electroweak correction [5] and $\ell = e,\ \mu$. Following a common convention, $f_+(0) \equiv f_+^{K^0\pi^-}(0)$. The mode dependence is contained in the $\delta$ terms: the long-distance electromagnetic (EM) corrections, which depend on the meson charges and lepton masses and the SU(2)-breaking corrections, which depend on the kaon species [6]. $I_{K\ell}$ is the integral of the dimensionless Dalitz-plot density $\rho(z, y)$ over the physical region for non radiative decays and includes $|\tilde{f}_{+,0}(t)|^2$. $z,\ y$ are the dimensionless pion and lepton energies $(=2E_{\pi,\ell}/M)$ and $\int \rho(z, y)\mathrm{d}z\,\mathrm{d}y = 1/4$ for all masses vanishing and all FF$=1$. $I_{K\ell}$ does not account for virtual and real radiative effects, which are included in $\delta_{K\ell}^{\mathrm{EM}}$.

The experimental inputs to eq. 2.3 are the semileptonic decay rates, *i.e.* branching ratios (BR) and lifetimes, and the reduced form factors $\tilde{f}_+(t)$ and $\tilde{f}_0(t)$, whose behavior as a function of $t$ is obtained from the decay pion spectra. At the current level of experimental precision, the choice of parametrization of the form-factor $t$ dependence becomes a relevant issue, as discussed below.

If the form factors are expanded in powers of $t$ up to $t^2$ as

$$\tilde{f}_{+,0}(t) = 1 + \lambda'_{+,0}\,\frac{t}{m^2} + \frac{1}{2}\,\lambda''_{+,0}\,\left(\frac{t}{m^2}\right)^2, \qquad (2.4)$$

four parameters ($\lambda'_+$, $\lambda''_+$, $\lambda'_0$ and $\lambda''_0$) need to be determined from the decay pion spectrum in order to be able to compute the phase-space integral. However, this parametrization of the form factors is problematic, because the values for the $\lambda$s obtained from fits to the experimental decay spectrum are strongly correlated, as discussed in ref. [7]. In particular, the correlation between $\lambda'_0$ and $\lambda''_0$ is $-99.96\%$; that between $\lambda'_+$ and $\lambda''_+$ is $-97.6\%$. It is therefore impossible to obtain meaningful results using this parametrization.

Form factors can also by described by a pole form:

$$\tilde{f}_{+,0}(t) = \frac{M_{V,S}^2}{M_{V,S}^2 - t}, \qquad (2.5)$$

which expands to $1 + t/M_{V,S}^2 + (t/M_{V,S}^2)^2 + \ldots$. It is not obvious however what vector and scalar states should be used.

| $p_n$ | $\tilde{f}_+(t)$ | $\tilde{f}_0(t)$ |
|---|---|---|
| $p_2 \times 10^4$ | $5.84 \pm 0.93$ | $4.16 \pm 0.50$ |
| $p_3 \times 10^4$ | $0.30 \pm 0.02$ | $0.27 \pm 0.01$ |

**Table 1:** Constants appearing in the dispersive form of vector and scalar form factors.

Recent $K_{Le3}$ measurements [8 – 10] show that the vector form factor $f_+(t)$ is dominated by the nearest vector $(q\bar{q})$ state with one strange and one light quark (or $K\pi$ resonance, in an older language). The pole-fit results are also consistent with predictions from a dispersive approach [11 – 13]. We will therefore make use of a parametrization for the vector form factor based on a dispersion relation twice subtracted at $t = 0$ [12]:

$$\tilde{f}_+(t) = \exp\left[\frac{t}{m_\pi^2}\left(\Lambda_+ + H(t)\right)\right],\tag{2.6}$$

where $H(t)$ is obtained from $K\pi$ scattering data. An approximation to eq. 2.6 [11, 12] is

$$\tilde{f}_+(t) = 1 + \lambda_+\frac{t}{m^2} + \frac{\lambda_+^2 + p_2}{2}\left(\frac{t}{m^2}\right)^2 + \frac{\lambda_+^3 + 3p_2\lambda_+ + p_3}{6}\left(\frac{t}{m^2}\right)^3\tag{2.7}$$

with $\lambda_+ = \Lambda_+$. $p_2$ and $p_3$ are given in table 1, second column. The approximation is valid to $\mathcal{O}(10^{-3})$ or better.

The pion spectrum in $K_{\mu3}$ decay has also been measured recently [8, 14, 15]. As discussed above, there is no sensitivity to $\lambda_0''$. All authors have fitted their data using a linear parametrization for the scalar form factor:

$$\tilde{f}_0(t) = 1 + \lambda_0'\frac{t}{m^2}.\tag{2.8}$$

Because of the strong correlation between $\lambda_0'$ and $\lambda_0''$, use of the linear rather than the quadratic parametrization gives a value for $\lambda_0'$ which is greater that the correct value by an amount equal to about 3.5 times the value of $\lambda_0''$. To clarify this situation, it is necessary to obtain a form for $\tilde{f}_0(t)$ with at least $t$ and $t^2$ terms but with only one parameter.

The Callan-Treiman relation [16] fixes the value of scalar FF at $t = \Delta_{K\pi}$ (the so-called Callan-Treiman point) to the ratio of the pseudoscalar decay constants $f_K/f_\pi$. This relation is slightly modified by SU(2)-breaking corrections [17]:

$$\tilde{f}_0(\Delta_{K\pi}) = \frac{f_K}{f_\pi}\frac{1}{f_+(0)} + \Delta_{\text{CT}},\tag{2.9}$$

where $\Delta_{\text{CT}}$ is of $\mathcal{O}(10^{-3})$. A recent parametrization for the scalar form factor [11] allows the constraint given by the Callan-Treiman relation to be exploited. It is a twice-subtracted representation of the form factor at $t = \Delta_{K\pi}$ and $t = 0$:

$$\tilde{f}_0(t) = \exp\left[\frac{t}{\Delta_{K\pi}}(\ln C - G(t))\right],\tag{2.10}$$

such that $C = \tilde{f}_0(\Delta_{K\pi})$ and $\tilde{f}_0(0) = 1$. $G(t)$ is derived from $K\pi$ scattering data. As suggested in ref. [11], a good approximation to eq. 2.10 is

$$\tilde{f}_0(t) = 1 + \lambda_0 \frac{t}{m^2} + \frac{\lambda_0{}^2 + p_2}{2} \left(\frac{t}{m^2}\right)^2 + \frac{\lambda_0{}^3 + 3p_2\lambda_0 + p_3}{6} \left(\frac{t}{m^2}\right)^3 \qquad (2.11)$$

with $p_2$ and $p_3$ as given in table 1. The Taylor expansion gives $\ln C = \lambda_0 \Delta_{K\pi}/m_\pi^2 + (0.0398 \pm 0.0041)$. Eq. (2.11) is quite similar to the result in ref. [18].

## 2.2 $K \to \mu\nu$ decays

High-precision lattice quantum chromodynamics (QCD) results have recently become available and are rapidly improving [19]. The availability of precise values for the pion- and kaon-decay constants $f_\pi$ and $f_K$ allows use of a relation between $\Gamma(K_{\mu2})/\Gamma(\pi_{\mu2})$ and $|V_{us}|^2/|V_{ud}|^2$, with the advantage that lattice-scale uncertainties and radiative corrections largely cancel out in the ratio [20]:

$$\frac{\Gamma(K_{\mu2(\gamma)})}{\Gamma(\pi_{\mu2(\gamma)})} = \frac{|V_{us}|^2}{|V_{ud}|^2} \frac{f_K^2}{f_\pi^2} \frac{m_K \left(1 - m_\mu^2/m_K^2\right)^2}{m_\pi \left(1 - m_\mu^2/m_\pi^2\right)^2} \times (0.9930 \pm 0.0035), \qquad (2.12)$$

where the uncertainty in the numerical factor is dominantly from structure-dependent radiative corrections and may be improved. Thus, it could very well be that the abundant decays of pions and kaons to $\mu\nu$ ultimately give the most accurate determination of the ratio of $|V_{us}|$ to $|V_{ud}|$. This ratio can be combined with direct measurements of $|V_{ud}|$ to obtain $|V_{us}|$. What is more interesting, however, is to combine all information from $\pi_{\mu2}$, $K_{e2}$, $K_{\mu2}$, $K_{e3}$, $K_{\mu3}$ and superallowed $0^+ \to 0^+$ nuclear $\beta$ decays to experimentally test electron-muon and lepton-quark universality, in addition to the unitarity of the quark mixing matrix.

## 3. KLOE at DAΦNE

The KLOE detector is operated at DAΦNE, the Frascati $\phi$ factory. DAΦNE is an $e^+e^-$ collider running at a center of mass energy $W = m_\phi \sim 1019.45$ MeV. $\phi$ mesons are produced with a cross section of $\sim 3$ $\mu$b and decay mostly to charged kaon pairs (49%) and neutral kaon pairs (34%).

The neutral kaon pair from $\phi \to K^0\bar{K}^0$ is in a pure $J^{PC} = 1^{--}$ state. Therefore the initial two-kaon state can be written, in the $\phi$-rest frame, as

$$|K\bar{K}, \ t=0\rangle = \left( \ |K^0(\mathbf{p}) \ \bar{K}^0(-\mathbf{p})\rangle - |\bar{K}^0(\mathbf{p}) \ K^0(-\mathbf{p})\rangle \ \right)/\sqrt{2}$$
$$\equiv \left( \ |K_S(\mathbf{p}) \ K_L(-\mathbf{p})\rangle - |K_L(\mathbf{p}) \ K_S(-\mathbf{p})\rangle \ \right)/\sqrt{2}, \qquad (3.1)$$

where the identity holds even without assuming $CPT$ invariance. Detection of a $K_S$ thus signals the presence of, "tags", a $K_L$ and vice versa. Thus at DAΦNE we have pure $K_S$ and $K_L$ beams of precisely known momenta (event by event) and flux, which can be used to measure absolute $K_S$ and $K_L$ branching ratios. In particular DAΦNE produces the only true pure $K_S$ beam and the only $K_L$ beam of known momentum. A $K_S$ beam
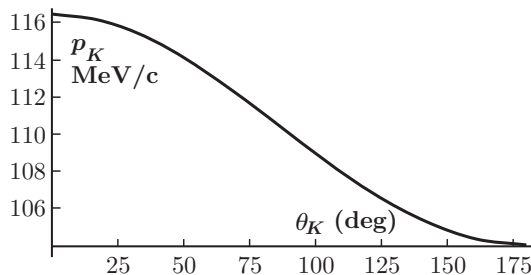
**Figure 2:** $K^0$-meson laboratory momentum vs angle to the $x$-axis.

permits studies of suppressed $K_S$ decays without overwhelming background from the $K_L$ component. A $K_L$ beam allows lifetime measurements. Similar arguments hold for $K^+$ and $K^-$ as well, although it is not hard to produce pure, monochromatic charged kaon beams.

In most of the following, kinematical variables will be needed in the kaon rest frame. At DAΦNE the collision center of mass, the $\phi$-meson rest frame, is not at rest in the laboratory. Electrons and positrons collide at an angle of $\pi$-0.025 radians. The $\phi$-mesons produced in the $e^+e^-$ collisions therefore move in the laboratory system toward the center of the accumulation rings with a momentum of about 13 MeV corresponding to $\beta_\phi{\sim}0.013$, $\gamma_\phi{=}{\sim}1.00008$. $K$ mesons from $\phi$-decay are therefore not monochromatic in the laboratory, figure 2. The $\phi$ momentum is measured run by run to high accuracy from Bhabha scattering. The neutral kaon momentum varies between $\sim$104 and $\sim$116 MeV and is a single valued function of the angle between the kaon momentum in the laboratory and the $\phi$ momentum, which we take as the $x$-axis. Knowledge of the kaon direction to a few degrees allows to return to the $\phi$-meson center of mass, figure 2. The mean charged kaon momentum is 127 MeV. Boosting the laboratory measured quantities to whichever frame is appropriate can therefore be done with great accuracy.

Because of all the above, KLOE is unique in that it is the only experiment that can at once measure the complete set of experimental inputs, branching ratios, lifetimes and FF parameters for the calculation of $|V_{us}|$ from both charged kaons and long lived neutral kaons. In addition KLOE is the only experiment that can measure $K_S$ branching ratios at the sub-percent level.

All following discussions refer to a system of coordinates with the $x$-axis in the horizontal plane, toward the center of DAΦNE, the $y$ axis vertical, pointing upwards and the $z$-axis bisecting the angle of the two beam lines. The origin is at the beams interaction point, IP.

## 4. The KLOE detector

At DAΦNE the mean $K_L$, $K_S$ and $K^\pm$ decay path lengths are $\lambda_L = 3.4$ m, $\lambda_S = 0.59$ cm and $\lambda_\pm = 95$ cm. A detector with a radius of $\sim$2 m is required to define a fiducial volume for the detection of $K_L$ decays with a geometrical efficiency of $\sim$30%. Figure 3 shows the vertical cross section of the KLOE detector in the $y$, $z$ plane. Because the radial distribution of the $K_L$ decay points is essentially uniform within this volume, tracks must
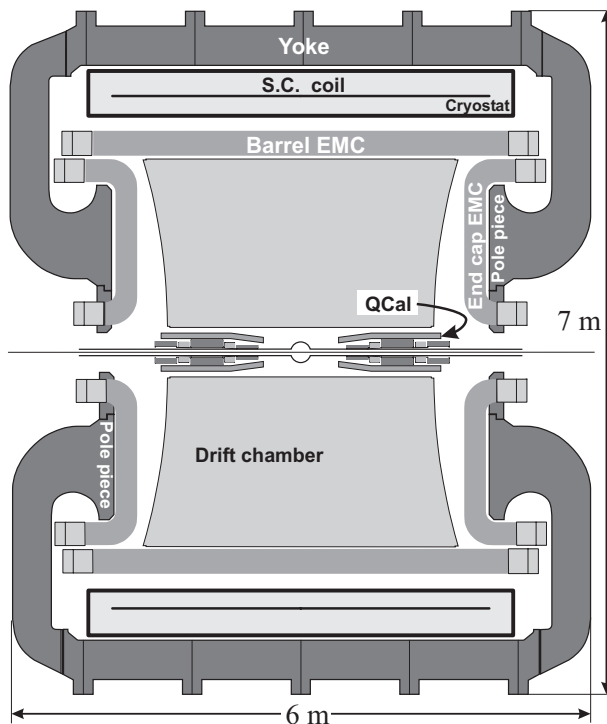
**Figure 3:** Vertical cross section of the KLOE detector.
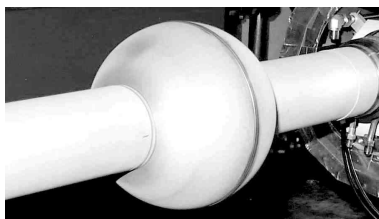


**Figure 4:** Beam pipe at the interaction point.

be well reconstructed independently of their angles of emission. In addition, the decay points of neutral particles to photons (e.g., $\pi^0 \rightarrow \gamma\gamma$) must be localized. To observe rare $K_S$ decays and $K_L K_S$ interference with no background from $K_S \rightarrow K_L$ regeneration, a decay volume around the interaction point with $r > 15\lambda_S$ must remain in vacuum. Material within the sensitive volume must be kept to a minimum to control regeneration, photon conversion, multiple scattering and energy loss for low-momentum charged particles. The beam pipe surrounds the interaction point, IP, with a sphere of 10 cm inner diameter, with walls 0.5 mm thick made of a Be-Al sintered compound. This sphere provides a vacuum path $\sim 8\times$ the $K_S$ *amplitude* decay length, effectively avoiding all $K_S \rightarrow K_L$ regeneration, see figure 4.

The detector consists principally of a large drift chamber (DC) surrounded by a hermetic electromagnetic calorimeter (EMC). A superconducting coil surrounding and supporting the calorimeter provides an axial magnetic field of 0.52 T.

The DC is 3.3 m long, with inner and outer radii of 25 and 200 cm, respectively.

It contains 12,582 drift cells arranged in 58 stereo layers uniformly filling the sensitive volume, for a total of 52,140 wires. The chamber uses a gas mixture of 90% helium and 10% isobutane. This reduces regeneration and multiple scattering within the chamber, while providing good spatial resolution (150 $\mu$m). Tracks from the origin with $\theta > 45°$ are reconstructed with $\sigma(p_\perp)/p_\perp \leq 0.4\%$ and two-track vertices within the sensitive volume are reconstructed with a position resolution of $\sim$3 mm. Signals from groups of 12 adjacent wires on each layer are added and digitized providing measurements of specific ionization. This allows identification of $K^\pm$ tracks by $dE/dx$ alone. The entire DC structure is built with carbon fiber composites to minimize photon conversion. A full description of the design and operation of the chamber can be found in ref. [21].

The calorimeter is built with cladded, 1 mm diameter scintillating fibers embedded in 0.5-mm-thick lead foils. The foils are imprinted with grooves just large enough to accommodate the fibers and some epoxy, without compressing the fibers thus preventing damage to the fiber-cladding interface. The epoxy provides structural strength and also removes light traveling in the cladding. Many such layers are stacked, glued and pressed, resulting in a material with a radiation length $X_0$ of 1.5 cm and an electromagnetic sampling fraction of $\sim$13%. This material is shaped into modules 23 cm thick ($\sim$15$X_0$).

24 modules of trapezoidal cross section are arranged in azimuth to form the calorimeter barrel and an additional 32 modules of square or rectangular cross section are wrapped around each of the pole pieces of the magnet yoke to form the endcaps. The unobstructed solid-angle coverage of the calorimeter as viewed from the origin is $\sim$94% of $4\pi$. The fibers run parallel to the axis of the detector in the barrel, while they are vertical in the endcaps, and are read out at both ends with a granularity of $4.4 \times 4.4$ cm$^2$ by a total of 4880 photomultiplier tubes, PM.

The PM signals provide the magnitude and time of energy deposits in the EMC. Deposits close in space and time are combined in clusters. Cluster energies are measured with a resolution of $\sigma_E/E = 5.7\%/\sqrt{E \text{ (GeV)}}$, as determined with the help of the DC using radiative Bhabha events. The time resolution is $\sigma_t = 57$ ps$/\sqrt{E \text{ (GeV)}}$ in quadrature with a constant term of 140 ps, as determined from radiative $\phi$ decays. The constant term results largely from the uncertainty on the collision time ($t_0$) arising from the length of the DA$\Phi$NE bunches. The constant contribution to the relative time resolution as determined using 2$\gamma$ events is $\sim$100 ps. Cluster positions are measured with resolutions of 1.3 cm in the coordinate transverse to the fibers and, by timing, of 1.2 cm$/\sqrt{E \text{ (GeV)}}$ in the longitudinal coordinate. These characteristics enable the 2$\gamma$ vertex in $K_L \rightarrow \pi^+\pi^-\pi^0$ decays to be localized with $\sigma \approx 2$ cm along the $K_L$ line of flight, as reconstructed from the tagging $K_S$ decay. The calorimeter is more fully described in ref. [22].

The data used for the measurements discussed in this paper were collected with a calorimeter trigger [23] requiring two energy deposits above a threshold of 50 MeV in the EMC barrel or 150 MeV in the endcaps. The KLOE trigger also implements logic to flag cosmic-ray events, which are recognized by the presence of two energy deposits above 30 MeV in the outermost calorimeter layers. For most KLOE data taking, such events were rejected after partial reconstruction by an online software filter.

At a luminosity of $10^{32}$ cm$^{-2}$s$^{-1}$, events are recorded at $\sim$2200 Hz. Of this rate,

~300 Hz are from $\phi$ decays. Raw data, reconstructed data and Monte Carlo (MC) events are stored in a tape library. Every run is reconstructed quasi-on-line, after a complete calibration of the entire detector and measurements of the DAΦNE parameters using the immediately preceding run. For a detailed description of the data acquisition, calibration, online and offline systems, see [24, 25].

In 2001–2002, KLOE collected an integrated luminosity of 450 pb$^{-1}$, corresponding to approximately 140 million tagged $K_S$ decays, 230 million tagged $K_L$ decays and 340 million tagged $K^{\pm}$ decays.

## 5. Kaon decay rate measurements

Equation (2.3) relates $|V_{us}|$ to the semileptonic kaon decay rates fully inclusive of radiation. One problem that consistently plagues the interpretation of older branching ratio measurements is the lack of clarity about accounting for radiative contributions. All of our measurements of kaon decays with charged particles in the final state are fully inclusive of radiation. Radiation is automatically accounted for in the acceptance correction. All our MC generators incorporate radiation as described in ref. [26].

### 5.1 $K_L$ decays

We search for $K_L$ decays using a beam tagged by detection of $K_S \to \pi^+\pi^-$ decays. The $\pi^+\pi^-$ decays observed near the origin count the number of $K_L$ mesons, providing the direction and momentum of each. We have used this technique to measure the BRs for the four main $K_L$ decay modes, as well as the $K_L$ lifetime [28, 29].

Once the $K_S \to \pi^+\pi^-$ decay is observed, we identify $K_L \to 3\pi^0$ decays by the presence of multiple photons reaching the calorimeter with arrival times consistent with a unique origin along the known $K_L$ flight path. We detect $K_L$ decays to charged modes ($\pi e\nu$, $\pi\mu\nu$ and $\pi^+\pi^-\pi^0$) primarily by the observation of two tracks forming a vertex along the $K_L$ path. We distinguish different decay modes by use of a single variable: the smaller absolute value of the two possible values of $\Delta_{\mu\pi} = |\mathbf{p}_{\text{miss}}| - E_{\text{miss}}$, where $|\mathbf{p}_{\text{miss}}|$ and $E_{\text{miss}}$ are the missing momentum and energy in the $K_L$ decay, evaluated assuming the decay particles are a $\pi^+\mu^-$ or a $\pi^-\mu^+$ pair. Figure 5 shows an example of a $\Delta_{\mu\pi}$ distribution. We obtain the numbers of $K_{e3}$, $K_{\mu3}$ and $\pi^+\pi^-\pi^0$ decays by fitting the $\Delta_{\mu\pi}$ spectrum with the appropriate MC-predicted shapes. A total of approximately 13 million tagged $K_L$ decays (328 pb$^{-1}$) are used for the measurement of the BRs [28].

Since the geometrical efficiency for detecting $K_L$ decays in the fiducial volume chosen depends on the $K_L$ lifetime $\tau_L$, so do the values of the four BRs. In our measurement:

$$\text{BR}(K_L \to f)/\text{BR}_0(K_L \to f) = 1 + 0.0128 \text{ ns}^{-1} \ (\tau_L - \tau_{L,0}), \qquad (5.1)$$

where $\text{BR}_0$ is the value of the branching ratio evaluated for a value $\tau_{L,0}$ of the $K_L$ meson lifetime. Our values of $\text{BR}_0$ for each mode and for a reference value of the lifetime $\tau_{L,0} = 51.54$ ns, the 1972 measurement of the $K_L$ lifetime [27], are listed in table 2. The four relations defined by eq. 5.1, together with the condition that the sum of all $K_L$ BRs must equal unity, allow the determination of the $K_L$ lifetime and the four BR values. This
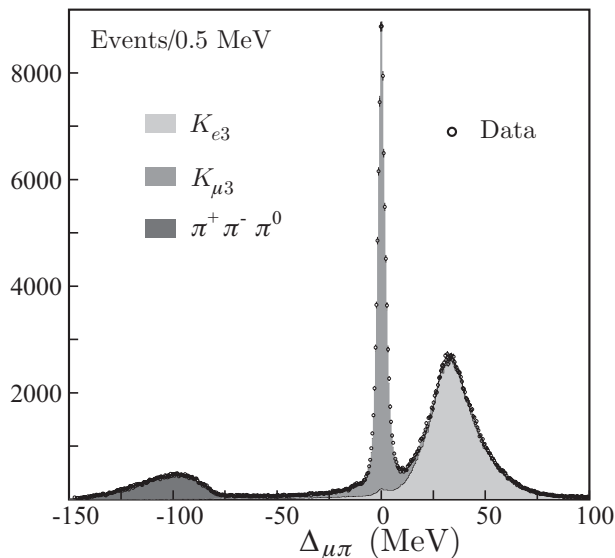
**Figure 5:** Distribution of $\Delta_{\mu\pi}$ for a subsample of $K_L$ decays leaving two tracks in the DC. Magnifying the graph by $\sim 12\times$, the $K_L \to \pi^+\pi^-$ signal becomes visible at $\Delta_{\mu\pi} \sim -12\,\mathrm{MeV}$.

| Parameter | Value | Correlation coefficients | | | |
|---|---|---|---|---|---|
| $\mathrm{BR}_0(K_{e3})$ | 0.4049(21) | 1 | | | |
| $\mathrm{BR}_0(K_{\mu3})$ | 0.2726(16) | +0.09 | 1 | | |
| $\mathrm{BR}_0(3\pi^0)$ | 0.2018(24) | +0.07 | −0.03 | 1 | |
| $\mathrm{BR}_0(\pi^+\pi^-\pi^0)$ | 0.1276(15) | +0.49 | +0.27 | +0.07 | 1 |

**Table 2:** KLOE measurements of principal $K_L$ BRs assuming $\tau_L = 51.54$ ns.
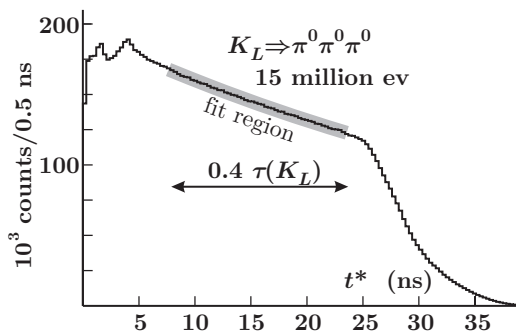


**Figure 6:** Proper-time distribution for $K_L \to 3\pi^0$ decays.

is the approach that we followed in ref. [28]. The final KLOE results, inclusive of other measurements are given below.

An additional, independent value for $\tau_L$ is obtained from the proper decay-time distribution for $K_L \to 3\pi^0$ events, figure 6, for which the reconstruction efficiency is high and uniform over a proper time interval of $\sim 0.4\,\tau_L$ [29], figure 6. About 8.5 million decays are observed within the proper-time interval $6.0 - 24.8$ ns; from a fit to the decay distribution we obtain $\tau_L = 50.92 \pm 0.17_{\mathrm{stat}} \pm 0.25_{\mathrm{syst}}$ ns.

| Parameter | Value | Correlation coefficients | | | | | | |
|---|---|---|---|---|---|---|---|---|
| BR($K_{e3}$) | 0.4008(15) | | | | | | | |
| BR($K_{\mu3}$) | 0.2699(14) | −0.31 | −0.00 | | | | | |
| BR($3\pi^0$) | 0.1996(20) | −0.55 | −0.41 | | | | | |
| BR($\pi^+\pi^-\pi^0$) | 0.1261(11) | −0.01 | −0.14 | −0.47 | | | | |
| BR($\pi^+\pi^-$) | $1.96(2) \times 10^{-3}$ | −0.15 | 0.50 | −0.21 | −0.07 | | | |
| BR($\pi^0\pi^0$) | $8.49(9) \times 10^{-4}$ | −0.15 | 0.48 | −0.20 | −0.07 | 0.97 | | |
| BR($\gamma\gamma$) | $5.57(8) \times 10^{-4}$ | −0.37 | −0.28 | 0.68 | −0.32 | −0.14 | −0.13 | |
| $\tau_L$ | 50.84(23) ns | 0.16 | 0.22 | −0.14 | −0.26 | 0.11 | 0.11 | −0.09 |

**Table 3:** Final KLOE measurements of principal $K_L$ BRs and $\tau_L$.

This latter measurement is included together with the results of table 2 in a fit to determine the $K_L$ BRs and lifetime. Note that the results in table 2 are obtained without assigning any error to $\tau_L$. We also use the KLOE result for BR($K_L \to \pi^+\pi^-(\gamma)$)/BR($K_{L\mu3}$) [30] and BR($K_L \to \gamma\gamma$)/BR($K_L \to 3\pi^0$) [31], requiring that the seven largest $K_L$ BRs add to unity. The only non-KLOE input to the fit is the 2006 PDG ETAFIT result BR($K_L \to \pi^0\pi^0$)/BR($K_L \to \pi^+\pi^-$) = 0.4391 ± 0.0013, based on relative amplitude measurements for $K \to \pi\pi$. We adjust this value to include direct emission in the $\pi^+\pi^-$ mode. There are thus eight experimental inputs, eight free parameters and one constraint. The results of the fit are presented in table 3; the fit gives $\chi^2$/dof=0.19/1 (CL=66%). The BRs for the $K_{Le3}$ and $K_{L\mu3}$ decays are determined to within 0.4% and 0.5%, respectively.

### 5.2 $K_S$ decays

We have measured the ratios BR($K_S \to \pi e\nu$)/BR($K_S \to \pi^+\pi^-$) separately for each lepton charge, using $\phi \to K_L K_S$ decays in which the $K_L$ is recognized by its interaction in the calorimeter barrel. Semileptonic $K_S$ decays are identified by time of flight (TOF) of both pion and electron. Our most recent analysis [32] gives about 13,600 signal events, expanding upon the statistics of our original measurement [33] by a factor of 22. Figure 7 shows the distributions of $E_{\rm miss} - |\mathbf{p}_{\rm miss}|$ for $K_{e3}$ event candidates. This quantity is zero for signal events which contain an unobserved neutrino. The signal peak is prominent and well separated from the background. Combining the data for both charges we obtain BR($K_S \to \pi e\nu$)/BR($K_S \to \pi^+\pi^-$)=(10.19 ± 0.11$_{\rm stat}$ ± 0.07$_{\rm syst}$) × $10^{-4}$ [32]. We also obtain the first measurement of the $K_S$ semileptonic charge asymmetry, $A_S = (1.5 \pm 9.6_{\rm stat} \pm 2.9_{\rm syst}) \times 10^{-3}$.

In a separate analysis, we have used $K_S$ decays tagged by the $K_L$ interaction in the EMC barrel to measure BR($K_S \to \pi^+\pi^-$)/BR($K_S \to \pi^0\pi^0$) = 2.2549 ± 0.0054 [34], where this value includes a previous KLOE result [35]. Together, these measurements completely determine the main $K_S$ BRs and give: BR($K_S \to \pi e\nu$)=(7.046 ± 0.091) × $10^{-4}$ [32].

In our evaluation of $|V_{us}|$, we use the KLOE value for BR($K_S \to \pi e\nu$) together with the lifetime value $\tau_S = 0.08958 \pm 0.00005$ ns from the PDG fit to $CP$ parameters [3]. This lifetime value is mostly due to measurements from NA48 [36] and KTeV [37].
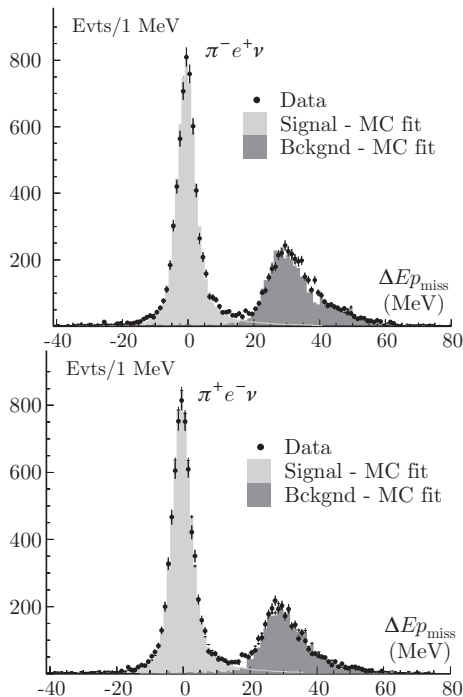
**Figure 7:** Distributions in $E_{\text{miss}} - p_{\text{miss}}$ (evaluated in the signal mass hypothesis) for candidate (top) $K_S \to \pi^- e^+ \nu$ and (bottom) $K_S \to \pi^+ e^- \bar{\nu}$ events.
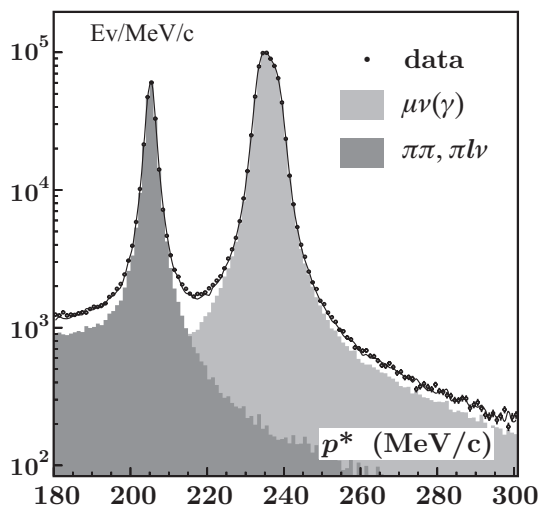


**Figure 8:** Distribution of $p^*$, the charged particle momentum in the kaon rest frame, for $K^\pm$ decays. The solid line is the sum of all contributions, in grey, from data control samples.

## 5.3 $K^\pm$ decays

At KLOE, $\phi \to K^+ K^-$ events are identified by detecting the abundant two-body decay $(\text{BR}(K^\pm \to \pi^\pm \pi^0 + K^\pm \to \mu^\pm \nu) \sim 84\%)$ of one of the kaons. As in the analysis of neutral kaon decays, this provides tagging of the kaon of opposite charge. As noted above, the decay $K \to \mu\nu$ is of interest in its own right for the determination of $|V_{us}|$.

Charged kaon decays are observed as "kinks" in a track originating at the IP. The
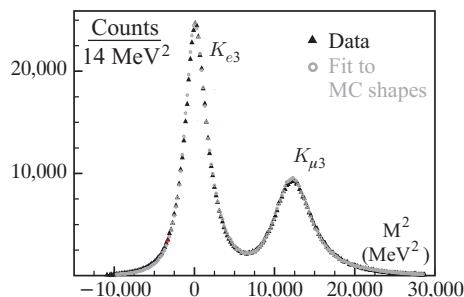
**Figure 9:** Distribution of $m_\ell^2$, from TOF information, for $K_{\ell 3}^\pm$ events.

charged kaon track must satisfy $70 < p < 130\,\mathrm{MeV}$. The momentum of the decay particle in the kaon rest frame, $p^*$, is 205 and 236 MeV, for $K^\pm$ decays to $\pi^\pm\pi^0$ and $\mu^\pm\nu$, respectively. Figure 8 shows the $p^*$ distribution obtained assuming that the decay particle is a pion. The shaded regions indicate contributions to the $p^*$ distribution as evaluated from data control samples. The peak for $K \to \mu\nu$ decays, although distorted because of the use of the wrong mass, remains clearly visible.

We measure $\mathrm{BR}(K^+ \to \mu^+\nu)$ (and also $\mathrm{BR}(K^+ \to \pi^+\pi^0)$, [38]) using $K^- \to \mu^-\bar\nu$ decays as tags, see [39] for details. We obtain the numbers of $\mu\nu$ and $\pi\pi^0$ events from the $p^*$ distribution for tagged events, as in figure 8. In $\sim$34% of some four million tagged events, we find $\sim$865,000 signal events with $225 \leq p^* \leq 400$ MeV, giving $\mathrm{BR}(K^+ \to \mu^+\nu(\gamma)) = 0.6366 \pm 0.0009_{\mathrm{stat}} \pm 0.0015_{\mathrm{syst}}$, using efficiencies from MC and control samples. This measurement is fully inclusive of final-state radiation (FSR), has a 0.27% uncertainty and is independent of the charged kaon lifetime.

To measure $\mathrm{BR}(K_{e3}^\pm)$ and $\mathrm{BR}(K_{\mu3}^\pm)$, we use both $K \to \mu\nu$ and $K \to \pi\pi^0$ decays as tags. We measure the semileptonic BRs separately for $K^+$ and $K^-$. Therefore, $\mathrm{BR}(K_{e3})$ and $\mathrm{BR}(K_{\mu3})$ are each determined from four independent measurements ($K^+$ and $K^-$ decays; $\mu\nu$ and $\pi\pi^0$ tags). Two-body decays are removed from the sample by kinematics, as described above. We then require that the TOF of the photons from the $\pi^0$ decay are consistent with the $K \to \ell$ decay point. Finally, from the TOF and momentum measurement for the lepton tracks, we obtain the $m_\ell^2$ distribution shown in figure 9.

The number of signal events for the two channels, plus residual background, is found fitting the $m_\ell^2$ distribution with the Monte Carlo predicted shapes. In all, we find about 300,000 $K_{e3}$ and 160,000 $K_{\mu3}$ events. We obtain consistent values of the BR for each decay from each of the four subsamples; when averaged we obtain $\mathrm{BR}_0(K_{e3}) = (4.965 \pm 0.038_{\mathrm{stat}} \pm 0.037_{\mathrm{syst}})\%$ and $\mathrm{BR}_0(K_{\mu3}) = (3.233 \pm 0.029_{\mathrm{stat}} \pm 0.026_{\mathrm{syst}})\%$, with a correlation of 62.7%. Further details are given on [40].

The above BRs are evaluated using the current world average value for the $K^\pm$ lifetime, $\tau_{\pm,0} = 12.385$ ns [3]. The BRs depend on the value assumed for $\tau_\pm$. In our measurement:

$$\mathrm{BR}(K^\pm \to f)/\mathrm{BR}_0(K^\pm \to f) = 1 - 0.0364\ \mathrm{ns}^{-1}\ (\tau_\pm - \tau_{\pm,0}). \qquad (5.2)$$

This dependence is used in the final evaluation of $\mathrm{BR}(K^\pm \to f)$.

| Parameter | Value | Correlation coefficients | | |
|---|---|---|---|---|
| $\mathrm{BR}(K_{e3})$ | 0.04972(53) | 1 | | |
| $\mathrm{BR}(K_{\mu3})$ | 0.03237(39) | $+0.63$ | 1 | |
| $\tau_\pm$ | 12.347(30) ns | $-0.10$ | $-0.09$ | 1 |

**Table 4:** KLOE measurements of $K^\pm$ semileptonic decays and lifetime.

The average value [3], for the lifetime of the charged kaon is nominally quite precise: $\tau_\pm = 12.385 \pm 0.025$ ns. However, the consistency of the input measurements is poor: the confidence level for the average is 0.2% and the error is scaled by 2.1. In addition the most precise result, see [41], quotes statistical errors which are less than half of the values which follow from the given number of events. It is quite important to confirm the value of $\tau_\pm$.

At KLOE, two methods are used to reconstruct the proper decay time distribution for charged kaons. The first is to obtain the decay time from the kaon path length in the DC, accounting for the continuous change in the kaon velocity due to ionization energy losses. A fit to the proper-time distribution in the interval from 15–35 ns ($1.6\lambda_\pm$) gives the result $\tau_\pm = 12.364 \pm 0.031_{\mathrm{stat}} \pm 0.031_{\mathrm{syst}}$ ns. Alternately, the decay time can be obtained from the precise measurement of the arrival times of the photons from $K^+ \to \pi^+\pi^0$ decays. In this case, a fit to the proper-time distribution in the interval from 13–42 ns ($2.3\lambda_\pm$) gives the result $\tau_\pm = 12.337 \pm 0.030_{\mathrm{stat}} \pm 0.020_{\mathrm{syst}}$ ns. For all fits we have a CL of $\sim$50% and excellent agreement between largely independent measurements. Taking into account the statistical correlation between these two measurements ($\rho = 0.307$), we obtain the average value $\tau_\pm = 12.347 \pm 0.030$ ns, see [42]. Inserting our result for $\tau_\pm$ into eqs. 5.2, we obtain the values of $K^\pm$ semileptonic BRs listed in table 4, which we use in our evaluation of $|V_{us}|$.

## 6. Form factor parameters for semileptonic $K_L$ decays

To measure the $K_{e3}$ form factor parameters [10], we start from the same sample of $K_L$ decays to charged particles used to measure the main $K_L$ BRs. We impose additional, loose kinematic cuts and make use of time of flight (TOF) information from the calorimeter clusters associated to the daughter tracks to obtain better particle identification (PID). The result is a high-purity sample of 2 million $K_L \to \pi e \nu$ decays. Within this sample, the identification of the electron and pion tracks is certain, so that the momentum transfer $t$ can be safely evaluated from the momenta of the $K_L$ and the daughter tracks. We obtain the vector form factor parameters from binned log-likelihood fits to the $t$ distribution. Using the quadratic parametrization of eq. 2.4, we obtain $\lambda'_+ = (25.5 \pm 1.5_{\mathrm{stat}} \pm 1.0_{\mathrm{syst}}) \times 10^{-3}$ and $\lambda''_+ = (1.4 \pm 0.7_{\mathrm{stat}} \pm 0.4_{\mathrm{syst}}) \times 10^{-3}$, where the total errors are correlated with $\rho = -0.95$. Using the pole parametrization of eq. 2.5, we obtain $M_V = 870 \pm 6_{\mathrm{stat}} \pm 7_{\mathrm{syst}}$ MeV. Evaluation of the phase-space integral for $K_L \to \pi e \nu$ decays gives $0.15470 \pm 0.00042$ using the values of $\lambda'_+$ and $\lambda''_+$ from the first fit and $0.15486 \pm 0.00033$ using the value of $M_V$ from the second; these results differ by $\sim$0.1%, while both fits give $\chi^2$ probabilities of $\sim$92%. The results we obtain using quadratic and pole fits are manifestly consistent.

The measurement of the vector and scalar FF parameters using $K_L \to \pi\mu\nu$ decays is more complicated. As noted in section 2.1, there are two form factors to consider, and since all information about the structure of these form factors is contained in the distribution of pion energy (or equivalently, $t$), the correlations between FF parameters are very large. In particular, it is not possible to measure $\lambda_0''$ for any conceivable number of events [7]. In addition, at KLOE energies clean and efficient $\pi/\mu$ separation is much more difficult to obtain than good $\pi/e$ separation. However, the FF parameters may also be obtained from fits to the distribution of the neutrino energy $E_\nu$ after integration over the pion energy. $E_\nu$ is simply the missing momentum in the $K_L \to \pi\mu\nu$ decay evaluated in the $K_L$ rest frame and no $\pi/\mu$ identification is required to calculate it. A price is paid in statistical sensitivity: the $E_\nu$ distribution is related to the $t$ distribution via an integration over the pion energy. As a result the statistical errors on the FF parameters will be 2–3 times larger when fitting the $E_\nu$ spectrum, rather than the $E_\pi$ spectrum. This is the case if the fit parameters are $\lambda_+'$, $\lambda_+''$ and $\lambda_0'$.

For this analysis [43], we start from the same sample of tagged $K_L$ decays to charged particles discussed above. We impose kinematic cuts that are tighter than those used for the $K_{e3}$ analysis and make use of shower profile information to augment the power of the PID cuts based on the TOF measurements for associated calorimeter clusters. We obtain a sample of about 1.8 million $K_L \to \pi\mu\nu$ decays with a residual contamination of $\sim 2.5\%$, flat in $E_\nu$. We first fit the $E_\nu$ distribution using eqs. 2.4 and (2.8) for the vector and scalar form factors. The result of this fit is [43]:

$$
\begin{array}{ll}
\lambda_+' = (22.3 \pm 9.8_{\text{stat}} \pm 3.7_{\text{syst}}) \times 10^{-3} & \\
\lambda_+'' = (4.8 \pm 4.9_{\text{stat}} \pm 1.6_{\text{syst}}) \times 10^{-3} & \begin{pmatrix} 1 & -0.97 & 0.81 \\ & 1 & -0.91 \\ & & 1 \end{pmatrix} \\
\lambda_0' = (9.1 \pm 5.9_{\text{stat}} \pm 2.6_{\text{syst}}) \times 10^{-3} &
\end{array}
\tag{6.1}
$$

with $\chi^2/\text{dof} = 19/29$. The correlation coefficients are given as a matrix. We then combine the above results with those from our $K_{e3}$ analysis, by a $\chi^2$ fit (statistical and systematic errors are combined). We find:

$$
\begin{array}{ll}
\lambda_+' = (25.6 \pm 1.7) \times 10^{-3} & \\
\lambda_+'' = (1.5 \pm 0.8) \times 10^{-3} & \begin{pmatrix} 1 & -0.95 & 0.29 \\ & 1 & -0.38 \\ & & 1 \end{pmatrix} \\
\lambda_0' = (15.4 \pm 2.2) \times 10^{-3} &
\end{array}
\tag{6.2}
$$

with $\chi^2/\text{dof} = 2.3/2$ and, once again, the correlation coefficients as given in the matrix. The same combination of $K_{e3}$ and $K_{\mu3}$ results has also been obtained using the dispersive representations of the form factors, eqs. 2.6 and (2.10), using the expansions of eqs. 2.7 and (2.11). Vector and scalar form factors are now described by just the $\lambda_+$ and $\lambda_0$ parameters. We find

$$
\begin{array}{l}
\lambda_+ = (25.7 \pm 0.4_{\text{stat}} \pm 0.4_{\text{syst}} \pm 0.2_{\text{param}}) \times 10^{-3} \\
\lambda_0 = (14.0 \pm 1.6_{\text{stat}} \pm 1.3_{\text{syst}} \pm 0.2_{\text{param}}) \times 10^{-3}
\end{array}
\tag{6.3}
$$

with $\chi^2/\text{dof} = 2.6/3$ and a correlation coefficient of $-0.26$. The uncertainties arising from the choice of parametrization for the vector and scalar form factors are given explicitly.

| Parameters | $I(K_{e3}^0)$ | $I(K_{\mu3}^0)$ | $I(K_{e3}^+)$ | $I(K_{\mu3}^+)$ |
|---|---|---|---|---|
| $\lambda'_+, \lambda''_+, \lambda'_0$ | 0.15483(40) | 0.10271(52) | 0.15919(41) | 0.10568(54) |
| $\lambda_+, \lambda_0$ | 0.15477(35) | 0.10262(47) | 0.15913(36) | 0.10559(48) |
| $\Delta$ (%) | 0.04 | 0.09 | 0.04 | 0.09 |

**Table 5:** Phase-space integrals for $K_{\ell3}$ decays, using eqs. (6.2), (6.3). $\Delta$ is the fractional difference.

| Channel | $\delta_K^{\mathrm{SU(2)}}$ | $\delta_{K\ell}^{\mathrm{EM}}$ |
|---|---|---|
| $K_{e3}^0$ | 0 | 0.57(15)% |
| $K_{\mu3}^0$ | 0 | 0.80(15)% |
| $K_{e3}^\pm$ | 2.36(22)% | 0.08(15)% |
| $K_{\mu3}^\pm$ | 2.36(22)% | 0.05(15)% |

**Table 6:** Summary of SU(2)-breaking and EM corrections.

The values of the phase-space integrals for $K_{\ell3}$ decays are listed in table 5, for both values of the FF parameters, eqs. (6.2) and (6.3), together with their fractional differences $\Delta$. Use of the dispersive parametrization changes the value of the phase-space integrals by at most $\sim$0.09% with respect to the results obtained using quadratic and linear parametrizations for vector and scalar form factors. The larger change observed for $K_{\mu3}$ decays is due to the incorrect use of a linear form for the $\tilde{f}_0(t)$ FF which results in a larger value of $\lambda'_0$ [7] and a larger integral. We shall use the dispersive results in the following. The difference between results corresponds to $\sim$0.03% change in $|f_+(0)\,V_{us}|$.

From the Callan-Treiman relation, eq. 2.9, we find $f_+(0) = 0.967 \pm 0.025$, using $f_K/f_\pi = 1.189 \pm 0.007$ from a recent lattice calculation [44] and $\Delta_{\mathrm{CT}} = (-3.5 \pm 8.0) \times 10^{-3}$, [17]. The error on our result for $f_+(0)$ is almost entirely from the uncertainty on our measurement of $\lambda_0$. Our result for $f_+(0)$ can be compared with the currently most precise lattice determination, $f_+(0) = 0.9644 \pm 0.0049$ [45].

# 7. $|f_+(0)\,V_{us}|$ and lepton universality

The SU(2)-breaking and EM corrections used to evaluate $|f_+(0)\,V_{us}|$ are summarized in table 6. The SU(2)-breaking correction is evaluated with ChPT to $\mathcal{O}(p^4)$, as described in [46]. The long distance EM corrections to the full inclusive decay rate are evaluated with ChPT to $\mathcal{O}(e^2p^2)$ [46] using low-energy constants from ref. [47]. The entries in the table have been evaluated recently [48] and include for the first time the values of $\delta^{\mathrm{EM}}$ for the $K_{\mu3}$ channels for both neutral and charged kaons. Using all of the experimental and theoretical inputs discussed above, the values of $|f_+(0)\,V_{us}|$ have been evaluated for the $K_{Le3}$, $K_{L\mu3}$, $K_{Se3}$, $K_{e3}^\pm$, and $K_{\mu3}^\pm$ decay modes, as shown in table 7 and in figure 10. Statistical and systematic uncertainties are added in quadrature everywhere. The five different determinations have been averaged, taking into account all correlations. We find

$$|f_+(0)\,V_{us}| = 0.2157 \pm 0.0006 \tag{7.1}$$

| Channel | $\|f_+(0)\,V_{us}\|$ | Correlation coefficients | | | | |
|---|---|---|---|---|---|---|
| $K_{Le3}$ | 0.2155(7) | 1 | | | | |
| $K_{L\mu3}$ | 0.2167(9) | 0.28 | 1 | | | |
| $K_{Se3}$ | 0.2153(14) | 0.16 | 0.08 | 1 | | |
| $K^{\pm}_{e3}$ | 0.2152(13) | 0.07 | 0.01 | 0.04 | 1 | |
| $K^{\pm}_{\mu3}$ | 0.2132(15) | 0.01 | 0.18 | 0.01 | 0.67 | 1 |

**Table 7:** KLOE results for $\|f_+(0)\,V_{us}\|$.
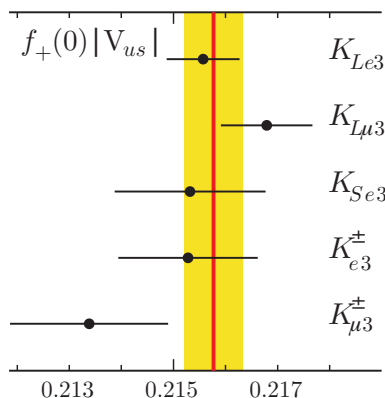


**Figure 10:** KLOE results for $\|f_+(0)\,V_{us}\|$.

with $\chi^2/\text{ndf} = 7.0/4$ (CL=13%). The values and the average are shown in figure 10. It is worth noting that the only external experimental input to this analysis is the $K_S$ lifetime. All other experimental inputs are KLOE results.

To evaluate the reliability of the SU(2)-breaking correction, we compare the separate averages of $\|f_+(0)\,V_{us}\|$ for the neutral and charged channels, which are 0.2159(6) and 0.2145(13), respectively. With correlations taken into account, these values agree to within $1.1\sigma$. Alternatively, an experimental estimate of $\delta^{\text{SU}(2)}$ can be obtained from the difference between the results for neutral and charged kaon decays, with no SU(2)-breaking corrections applied in the latter case. We obtain $\delta^{\text{SU}(2)}_{\text{exp}} = 1.67(62)\%$, which is in agreement with the value estimated from theory (table 6).

Comparison of the values of $\|f_+(0)\,V_{us}\|$ for $K_{e3}$ and $K_{\mu3}$ modes provides a test of lepton universality. Specifically,

$$r_{\mu e} \equiv \frac{\|f_+(0)\,V_{us}\|^2_{\mu3,\ \text{exp}}}{\|f_+(0)\,V_{us}\|^2_{e3,\ \text{exp}}} = \frac{\Gamma_{\mu3}}{\Gamma_{e3}}\ \frac{I_{e3}\,(1+\delta_{Ke})^2}{I_{\mu3}\,(1+\delta_{K\mu})^2}, \tag{7.2}$$

where $\delta_{K\ell}$ stands for $\delta^{\text{SU}(2)}_K + \delta^{\text{EM}}_{K\ell}$. By comparison with eq. 2.3, $r_{\mu e}$ is equal to the ratio $g^2_\mu/g^2_e$, with $g_\ell$ the coupling strength at the $W \to \ell\nu$ vertex. In the standard model, $r_{\mu e} = 1$. Averaging between charged and neutral modes, we find

$$r_{\mu e} = 1.000 \pm 0.008. \tag{7.3}$$

The sensitivity of this result may be compared with that obtained for $\pi \to \ell\nu$ decays, $(r_{\mu e})_\pi = 1.0042 \pm 0.0033$ [49], and for leptonic $\tau$ decays, $(r_{\mu e})_\tau = 1.000 \pm 0.004$ [50].
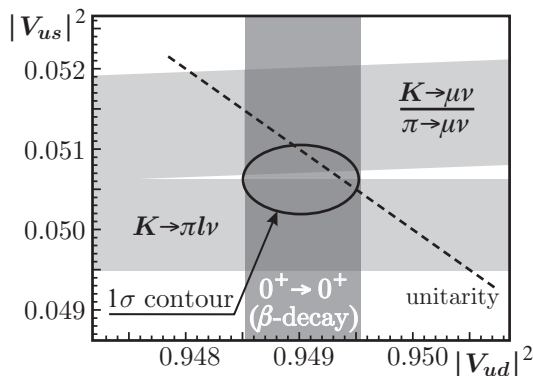
**Figure 11:** KLOE results for $|V_{us}|^2$, $|V_{us}/V_{ud}|^2$ and $|V_{ud}|^2$ from $\beta$-decay measurements, shown as $2\sigma$ wide grey bands. The ellipse is the $1\,\sigma$ contour from the fit. The unitarity constraint is illustrated by the dashed line.

## 8. Test of CKM unitarity

In the previous section, a determination of $|f_+(0)\,V_{us}|$ from $K_{\ell 3}$ decays has been obtained, with fractional accuracy of 0.28%. Lattice evaluations of $f_+(0)$ are rapidly improving in precision. The RBC and UKQCD Collaborations have recently obtained $f_+(0) = 0.9644 \pm 0.0049$ from a lattice calculation with $2+1$ flavors of dynamical domain-wall fermions [45]. Using their value for $f_+(0)$, our $K_{\ell 3}$ results give $|V_{us}| = 0.2237 \pm 0.0013$. A recent evaluation of $|V_{ud}|$ from $0^+ \to 0^+$ nuclear beta decays [51], gives $|V_{ud}| = 0.97418 \pm 0.00026$ which, combined with our result above, gives $|V_{ud}|^2 + |V_{us}|^2 - 1 = -0.0009 \pm 0.0008$, a result compatible with unitarity, which is verified to $\sim 0.1\%$. Figure 11 shows a compendium of all the KLOE results.

Additional information is provided by the determination of the ratio $|V_{us}/V_{ud}|$, following the approach of eq. 2.12. From our measurements of $\mathrm{BR}(K_{\mu 2})$ and $\tau_\pm$ and using $\Gamma(\pi_{\mu 2})$ from ref. [3], we find $|V_{us}/V_{ud} \times f_K/f_\pi|^2 = 0.0765(4)$. Using the recent lattice determination of $f_K/f_\pi$ from the HPQCD/UKQCD collaboration, $f_K/f_\pi = 1.189 \pm 0.007$ [44], we obtain $|V_{us}/V_{ud}|^2 = 0.0541 \pm 0.0007$. The best estimate of $|V_{us}|^2$ and $|V_{ud}|^2$ can be obtained from a fit to the above ratio and our result $|V_{us}|^2 = 0.05002 \pm 0.00057$ together with the result $|V_{ud}|^2 = 0.9490 \pm 0.0005$ from superallowed $\beta$-decays. The fit gives $|V_{us}|^2 = 0.0506 \pm 0.0004$ and $|V_{ud}|^2 = 0.9490 \pm 0.0005$ with a correlation of 3%. The fit CL is 13% ($\chi^2/\mathrm{ndf} = 2.34/1$). The values obtained confirm the unitarity of the CKM quark mixing matrix as applied to the first row. We find

$$1 - |V_{us}|^2 - |V_{ud}|^2 = 0.0004 \pm 0.0007 \quad (\sim 0.6\sigma)$$

*i.e.* the unitarity condition is verified to $\mathcal{O}(0.1\%)$, see figure 11. In a more conventional form, the results of the fit are:

$$\begin{aligned}
|V_{us}| &= 0.2249 \pm 0.0010 \\
|V_{ud}| &= 0.97417 \pm 0.00026
\end{aligned} \tag{8.1}$$

Imposing unitarity as a constraint, $|V_{us}|^2 + |V_{ud}|^2 = 1$, on the values above and performing a constrained fit we find

$$
\begin{aligned}
|V_{us}| &= 0.2253 \pm 0.0007 \\
|V_{ud}| &= \sqrt{1 - |V_{us}|^2} = 0.97429 \pm 0.00017.
\end{aligned}
\tag{8.2}
$$

The correlation is of course $-100\%$ and $\chi^2/\mathrm{dof}=0.37/1$ corresponding to a CL of 54%.

One should also keep in mind that while lattice results for $f_+(0)$ and $f_K/f_\pi$ appear to be converging and are quoted with small errors there is still a rather large spread between different calculations. If we were to use instead $f_+(0) = 0.961 \pm 0.008$ as computed in [52] and still preferred by many authors, we find $|V_{us}| = 0.2258 \pm 0.0012$ which is less precise but satisfies more closely unitarity.

All above results are obtained from our coherent, complete and self-consistent set of parameters. We therefore do not include results from other recent measurements, e.g. NA48 and ISTRA+ [53, 54]. Furthermore we note that both experiments give ratios of partial widths that require external information from ref. [3], which could be incorrect, see ref. [55, 56].

## 9. Bounds on new physics from $K_{\mu2}$ decay

A particularly interesting test is the comparison between the values for $|V_{us}|$ obtained from helicity-suppressed $K_{\ell2}$ decays and helicity-allowed $K_{\ell3}$ decays. To reduce theoretical uncertainties and make use of the results discussed above, we exploit the ratio $\mathrm{BR}(K_{\mu2})/\mathrm{BR}(\pi_{\mu2})$ and study the quantity

$$
R_{\ell23} = \left| \frac{V_{us}(K_{\mu2})}{V_{us}(K_{\ell3})} \times \frac{V_{ud}(0^+ \to 0^+)}{V_{ud}(\pi_{\mu2})} \right|.
\tag{9.1}
$$

This ratio is unity in the SM, but would be affected by the presence of non-vanishing scalar or right-handed currents. A scalar current due to a charged Higgs exchange is expected to lower the value of $R_{\ell23}$, which becomes (see [57]):

$$
R_{\ell23} = \left| 1 - \frac{m_{K^+}^2}{m_{H^+}^2} \left( 1 - \frac{m_{\pi^+}^2}{m_{K^+}^2} \right) \frac{\tan^2\beta}{1 + \epsilon_0 \tan\beta} \right|.
\tag{9.2}
$$

with $\tan\beta$ the ratio of the two Higgs vacuum expectation values in the MSSM and $\epsilon_0 \approx 0.01$ [58]. Any effects of scalar currents on $0^+ \to 0^+$ nuclear transitions and $K_{\ell3}$ decays are expected to be insignificant and $|V_{us}|$ and $|V_{ud}|$ as estimated from these modes are assumed to satisfy the unitarity condition. A comparison of eq. (9.2) with experiment leads to the exclusion of some values of $m_{H^+}$, $\tan\beta$, see figure 12.

To evaluate $R_{\ell23}$, we fit our experimental data on $K_{\mu2}$ and $K_{\ell3}$ decays, using the lattice determinations of $f_+(0)$ and $f_K/f_\pi$ and the value of $|V_{ud}|$ discussed above as inputs. We obtain

$$
R_{\ell23} = 1.008 \pm 0.008,
\tag{9.3}
$$

which is $1\sigma$ above the standard model prediction. This measurement places bounds on the charged Higgs mass and $\tan\beta$. Figure 12 shows the region in the $\{m_{H^+}, \tan\beta\}$ plane
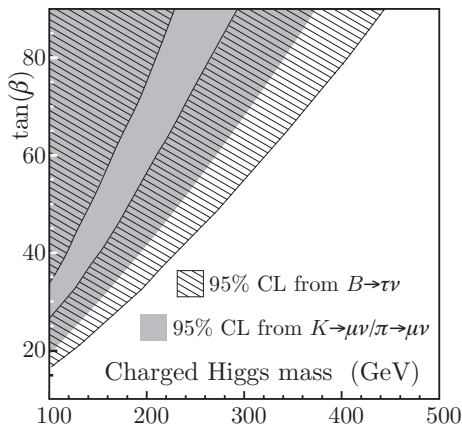
**Figure 12:** Region in the $m_{H^+}$-$\tan\beta$ plane excluded by our result for $R_{\ell 23}$; the region excluded by measurements of $\mathrm{BR}(B \to \tau\nu)$ is also shown.

excluded at 95% CL by our result for $R_{\ell 23}$. Measurements of $\mathrm{BR}(B \to \tau\nu)$ [59] also set bounds on $m_{H^+}$ and $\tan\beta$, as shown in the figure. While the $B \to \tau\nu$ data exclude an extensive region of the plane, there is an uncovered region corresponding to the change of sign of the correction. This region is fully covered by our result.

## 10. Conclusions

We have measured with very good accuracy all of the main $K_S$, $K_L$ and $K^+$ BRs, the $K_L$ and $K^+$ lifetimes, and the form factor parameters for semileptonic $K_L$ decays. We obtain $|f_+(0)\,V_{us}| = 0.2157 \pm 0.0006$ from a weighted average of the determinations for the $K_{Le3}$, $K_{L\mu3}$, $K_{Se3}$, $K_{e3}^{\pm}$ and $K_{\mu3}^{\pm}$ modes. We have also tested lepton universality in $K_{\ell 3}$ decays. We obtain $r_{\mu e} = 1.000 \pm 0.008$, a measurement of the ratio $g_\mu^2/g_e^2$ of the muon and electron gauge couplings. From our measurements of the $K_{\mu2}$ decay rate, we obtain $|V_{us}/V_{ud} \times f_K/f_\pi|^2 = 0.7650 \pm 0.0033$. Our determinations of both $|f_+(0)\,V_{us}|$ and $|V_{us}/V_{ud} \times f_K/f_\pi|$ have fractional uncertainties of $\sim 0.3\%$ and are comparable in precision to the present world averages [3].

Using recent lattice determinations for the meson form factors, we obtain $|V_{us}| = 0.2237 \pm 0.0013$ and $|V_{us}/V_{ud}| = 0.2326 \pm 0.0015$. We perform a fit to combine these values with the most recent evaluation of $|V_{ud}|$ from nuclear $\beta$ decays. The result of this fit satisfies the first-row CKM unitarity condition to within $0.6\sigma$ and gives $|V_{us}| = 0.2249 \pm 0.0010$ and $|V_{ud}| = 0.97417 \pm 0.00026$, unchanged from the input value. Imposing unitarity results in $|V_{us}| = 0.2253 \pm 0.0007$ and $|V_{ud}| = \sqrt{1 - |V_{us}|^2} = 0.97429 \pm 0.00017$ with a correlation of $-100\%$.

Comparing the values for $|V_{us}|$ obtained from $K_{\mu2}$ and $K_{\ell 3}$ decays, we are able to exclude a large region in the $\{m_{H^+},\, \tan\beta\}$ plane. The bounds from our measurements are complementary to those from results on $B \to \tau\nu$ decays.

## Acknowledgments

## References

[1] This paper is the beginning of the story, N. Cabibbo, *Unitary symmetry and leptonic decays*, *Phys. Rev. Lett.* **10** (1963) 531;
The mixing matrix for 6 flavors was first discussed by M. Kobayashi and T. Maskawa, *CP violation in the renormalizable theory of weak interaction*, *Prog. Theor. Phys.* **49** (1973) 652.

[2] C. Klopfenstein et al., *Semileptonic decay of the B meson*, *Phys. Lett.* **B 130** (1983) 444.

[3] PARTICLE DATA GROUP collaboration, W.M. Yao. et al., *Review of particle physics*, *J. Phys.* **G 33** (2006) 1 and 2007 web updates.

[4] M. Ademollo and R. Gatto, *Nonrenormalization theorem for the strangeness violating vector currents*, *Phys. Rev. Lett.* **13** (1964) 264.

[5] A. Sirlin, *Large $m(W)$, $m(Z)$ behavior of the $O(\alpha)$ corrections to semileptonic processes mediated by $W$*, *Nucl. Phys.* **B 196** (1982) 83.

[6] V. Cirigliano, M. Knecht, H. Neufeld, H. Rupertsberger and P. Talavera, *Radiative corrections to $K(l3)$ decays*, *Eur. Phys. J.* **C 23** (2002) 121 [hep-ph/0110153].

[7] P. Franzini, *Opening remarks*, PoS(KAON)002 (2007).

[8] KTEV collaboration, T. Alexopoulos et al., *Measurements of semileptonic $K(L)$ decay form factors*, *Phys. Rev.* **D 70** (2004) 092007 [hep-ex/0406003].

[9] NA48 collaboration, A. Lai et al., *Measurement of $K_0(e_3)$ form factors*, *Phys. Lett.* **B 604** (2004) 1 [hep-ex/0410065].

[10] KLOE collaboration, F. Ambrosino et al., *Measurement of the form-factor slopes for the decay $K(L) \to pi^{\pm}e^{\mp}\nu$ with the KLOE detector*, *Phys. Lett.* **B 636** (2006) 166 [hep-ex/0601038].

[11] V. Bernard, M. Oertel, E. Passemar and J. Stern, $K(L)(\mu_3)$ *decay: a stringent test of right-handed quark currents*, *Phys. Lett.* **B 638** (2006) 480 [hep-ph/0603202].

[12] V. Bernard, M. Oertel, E. Passmar and J. Stern, private communication. They compute a dispersion relation for $\ln f_+$ twice subtracted at $t = 0$, using $K\pi$ $p$-wave scattering data, as done in [11].

[13] M. Jamin, A. Pich and J. Portoles, *Spectral distribution for the decay tau $\to$ nu/tau K pi*, *Phys. Lett.* **B 640** (2006) 176 [hep-ph/0605096].

[14] NA48 collaboration, A. Lai et al., *Measurement of $K^0_{\mu3}$ form factors*, *Phys. Lett.* **B 647** (2007) 341 [hep-ex/0703002].

[15] O.P. Yushchenko et al., *High statistic study of the $K^- \to \pi_0 \mu^- \nu$ decay*, *Phys. Lett.* **B 581** (2004) 31 [hep-ex/0312004].

[16] C.G. Callan and S.B. Treiman, *Equal time commutators and K meson decays*, *Phys. Rev. Lett.* **16** (1966) 153.

[17] J. Gasser and H. Leutwyler, *Chiral perturbation theory: expansions in the mass of the strange quark*, *Nucl. Phys.* **B 250** (1985) 465.

[18] M. Jamin, J.A. Oller and A. Pich, *Scalar $K\pi$ form factor and light quark masses*, *Phys. Rev.* **D 74** (2006) 074009 [hep-ph/0605095].

[19] C. Davies, *Recent and future developments in lattice calculations*, talk at *Lepton-Photon '07 conference*, Daegu, Korea (2007).

[20] W.J. Marciano, *Precise determination of $|V(us)|$ from lattice calculations of pseudoscalar decay constants*, *Phys. Rev. Lett.* **93** (2004) 231803 [hep-ph/0402299].

[21] M. Adinolfi et al., *The tracking detector of the KLOE experiment*, *Nucl. Instrum. Meth.* **A488** (2002) 51.

[22] M. Adinolfi et al., *The KLOE electromagnetic calorimeter*, *Nucl. Instrum. Meth.* **A482** (2002) 364.

[23] KLOE collaboration, M. Adinolfi et al., *The trigger system of the KLOE experiment*, *Nucl. Instrum. Meth.* **A492** (2002) 134.

[24] A. Aloisio et al., *Data acquisition and monitoring for the KLOE detector*, *Nucl. Instrum. Meth.* **A516** (2004) 288.

[25] F. Ambrosino et al., *Data handling, reconstruction and simulation for the KLOE experiment*, *Nucl. Instrum. Meth.* **A534** (2004) 403 [physics/0404100].

[26] C. Gatti, *Monte Carlo simulation for radiative kaon decays*, *Eur. Phys. J.* **C 45** (2006) 417 [hep-ph/0507280].

[27] K.G. Vosburgh et al., *Measurement of the $K_0(L)$ mean life*, *Phys. Rev.* **D 6** (1972) 1834.

[28] KLOE collaboration, F. Ambrosino et al., *Measurements of the absolute branching ratios for the dominant $K(L)$ decays, the $K(L)$ lifetime and $V(us)$ with the KLOE detector*, *Phys. Lett.* **B 632** (2006) 43 [hep-ex/0508027].

[29] KLOE collaboration, F. Ambrosino et al., *Measurement of the $K(L)$ meson lifetime with the KLOE detector*, *Phys. Lett.* **B 626** (2005) 15 [hep-ex/0507088].

[30] KLOE collaboration, F. Ambrosino et al., *Measurement of the branching ratio of the $K(L) \to \pi^+\pi^-$ decay with the KLOE detector*, *Phys. Lett.* **B 638** (2006) 140 [hep-ex/0603041].

[31] KLOE collaboration, M. Adinolfi et al., *Measurement of the ratio* $\Gamma(K(L) \to \gamma\gamma)/\Gamma(K(L) \to \pi_0\pi_0\pi_0)$ *with the KLOE detector*, *Phys. Lett.* **B 566** (2003) 61 [hep-ex/0305035].

[32] KLOE collaboration, F. Ambrosino et al., *Measurement of the branching fraction and charge asymmetry for the decay* $K(S) \to \pi e\nu$ *with the KLOE detector*, *Phys. Lett.* **B 636** (2006) 173 [hep-ex/0601026].

[33] KLOE collaboration, A. Aloisio et al., *Measurement of the branching fraction for the decay* $K(S) \to \pi e\nu$, *Phys. Lett.* **B 535** (2002) 37 [hep-ph/0203232].

[34] KLOE collaboration, F. Ambrosino et al., *Precise measurement of* $\Gamma(K(S) \to \pi^+\pi^-(\gamma))/\Gamma(K(S) \to \pi_0\pi_0)$ *with the KLOE detector at DAFNE*, *Eur. Phys. J.* **C 48** (2006) 767 [hep-ex/0601025].

[35] KLOE collaboration, A. Aloisio et al., *Measurement of* $\Gamma(K(S) \to \pi^+\pi^-(\gamma))/\Gamma(K(S) \to \pi_0\pi_0)$, *Phys. Lett.* **B 538** (2002) 21 [hep-ex/0204024].

[36] NA48 collaboration, A. Lai et al., *A measurement of the* $K(S)$ *lifetime*, *Phys. Lett.* **B 537** (2002) 28 [hep-ex/0205008].

[37] KTeV collaboration, A. Alavi-Harati et al., *Measurements of direct CP-violation, CPT symmetry and other parameters in the neutral kaon system*, *Phys. Rev.* **D 67** (2003) 012005 [hep-ex/0208007].

[38] KLOE collaboration, F. Ambrosino et al., *The measurement of the absolute branching ratio of the* $K^+ \to \pi^+\pi_0(\gamma)$ *decay at KLOE*, arXiv:0707.2654.

[39] KLOE collaboration, F. Ambrosino et al., *Measurement of the absolute branching ratio for the* $K^+ \to \mu^+\nu(\gamma)$ *decay with the KLOE detector*, *Phys. Lett.* **B 632** (2006) 76 [hep-ex/0509045].

[40] KLOE collaboration and others, *Measurement of the absolute branching ratios for semileptonic* $K^\pm$ *decays with the KLOE detector*, *JHEP* **02** (2008) 098 [arXiv:0712.3841].

[41] R.J. Ott and T.W. Pritchard, *Precise measurement of the* $K^+$ *lifetime*, *Phys. Rev.* **D 3** (1971) 52.

[42] and others, *Measurement of the charged kaon lifetime with the KLOE detector*, *JHEP* **01** (2008) 073 [arXiv:0712.1112].

[43] KLOE collaboration, F. Ambrosino et al., *Measurement of the* $K_L \to \pi\mu\nu$ *form factor parameters with the KLOE detector*, *JHEP* **12** (2007) 105 [arXiv:0710.4470].

[44] HPQCD collaboration, E. Follana, C.T.H. Davies, G.P. Lepage and J. Shigemitsu, *High Precision determination of the* $\pi$, $K$, $D$ *and* $D_s$ *decay constants from lattice QCD*, *Phys. Rev. Lett.* **100** (2008) 062002 [arXiv:0706.1726].

[45] RBC/UKQCD collaboration, P.A. Boyle et al., $K(L_3)$ *semileptonic form factor from* $2+1$ *flavour lattice QCD*, arXiv:0710.5136.

[46] V. Cirigliano, M. Knecht, H. Neufeld, H. Rupertsberger and P. Talavera, *Radiative corrections to* $K(L_3)$ *decays*, *Eur. Phys. J.* **C 23** (2002) 121 [hep-ph/0110153].

[47] S. Descotes-Genon and B. Moussallam, *Radiative corrections in weak semi-leptonic processes at low energy: a two-step matching determination*, *Eur. Phys. J.* **C 42** (2005) 403 [hep-ph/0505077].

[48] V. Cirigliano, *Precision tests of the standard model with $K_{\ell_3}$ decays*, PoS(KAON)007 (2007).

[49] M.J. Ramsey-Musolf, S. Su and S. Tulin, *Pion leptonic decays and supersymmetry*, *Phys. Rev.* **D 76** (2007) 095017 [arXiv:0705.0028].

[50] M. Davier, A. Hocker and Z. Zhang, *The physics of hadronic $\tau$ decays*, *Rev. Mod. Phys.* **78** (2006) 1043 [hep-ph/0507078].

[51] I.S. Towner and J.C. Hardy, *An improved calculation of the isospin-symmetry-breaking corrections to superallowed Fermi beta decay*, *Phys. Rev.* **C 77** (2008) 025501 [arXiv:0710.3181].

[52] H. Leutwyler and M. Roos, *Determination of the elements $V(us)$ and $V(ud)$ of the Kobayashi-Maskawa matrix*, *Z. Physik* **C 25** (1984) 91.

[53] NA48/2 collaboration, J.R. Batley et al., *Measurements of charged kaon semileptonic decay branching fractions $K^\pm \to \pi^0 \mu^\pm \nu$ and $K^\pm \to \pi^0 e^\pm \nu$ and their ratio*, *Eur. Phys. J.* **C 50** (2007) 329 [hep-ex/0702015].

[54] V.I. Romanovsky et al., *Measurement of $K_{e3}^-$ branching ratio*, arXiv:0704.2052.

[55] M. Antonelli, *Precision tests of standard model with leptonic and semileptonic kaon decays*, arXiv:0712.0734.

[56] FLAVIANET WORKSHOP ON KAON DECAYS collaboration, M. Antonelli et al., *Precision tests of the standard model with leptonic and semileptonic kaon decays*, arXiv:0801.1817.

[57] G. Isidori and P. Paradisi, *Hints of large $\tan \beta$ in flavour physics*, *Phys. Lett.* **B 639** (2006) 499 [hep-ph/0605012].

[58] G. Isidori and A. Retico, *Scalar flavour-changing neutral currents in the large-$\tan \beta$ limit*, *JHEP* **11** (2001) 001 [hep-ph/0110121].

[59] K. Ikado et al., *Evidence of the purely leptonic decay $B^- \to \tau^- \bar{\nu}/\tau$*, *Phys. Rev. Lett.* **97** (2006) 251802 [hep-ex/0604018];
BABAR collaboration, B. Aubert et al., *A search for $B^+ \to \tau + \nu$*, *Phys. Rev.* **D 76** (2007) 052002 [arXiv:0705.1820].